



# Tumor Promoting Role of NRIP1 in Oral Squamous Cell Carcinoma: The Involvement of NSD2-Mediated Histone Methylation of DGCR8

Lili Zhang<sup>1</sup> and Guangyao Hu<sup>1</sup>

<sup>1</sup>Department of Stomatology, Affiliated Hospital of Beihua University, Jilin, Jilin, China

Oral squamous cell carcinoma (OSCC) remains the most prevalent malignance in the head and neck with highly aggressive attributes. This study investigates the functions of nuclear receptor interacting protein 1 (NRIP1) and its target transcripts in the progression of OSCC. By analyzing four OSCC-related Gene Expression Omnibus (GEO) datasets (GSE9844, GSE23558, GSE25104 and GSE74530) and querying bioinformatics systems, we obtained NRIP1 as an aberrantly highly expressed transcription factor in OSCC. Increased NRIP1 was detected in OSCC cell lines. Artificial downregulation of NRIP1 significantly suppressed proliferation, migration and invasion, resistance to apoptosis, tumorigenicity, and *in vivo* metastatic potential of OSCC cells. Moreover, the bioinformatics analyses suggested nuclear receptor binding SET domain protein 2 (NSD2) as a target of NRIP1 and DGCR8 microprocessor complex subunit (DGCR8) as a target of NSD2. Indeed, we validated by chromatin immunoprecipitation and luciferase assays that NRIP1 activated the transcription of NSD2, and NSD2 increased DGCR8 transcription by modulating histone methylation near the DGCR8 promoter. Either NSD2 or DGCR8 upregulation in OSCC cells rescued their malignant properties. Collectively, this study demonstrates that NRIP1 augments malignant properties of OSCC cells by activating NSD2-mediated histone methylation of DGCR8.

**Keywords:** DGCR8; histone methylation; NRIP1; NSD2; oral squamous cell carcinoma

Tohoku J. Exp. Med., 2023 July, 260 (3), 193-204.

doi: 10.1620/tjem.2023.J029

## Introduction

Head and neck squamous cell carcinoma (HNSCC) are the most prevailing malignancies that arise in the head and neck, and oral squamous cell carcinoma (OSCC) stands for the most common subtype of HNSCC and is featured with high metastasis and recurrence rates as well as treatment resistance (Yang et al. 2021). According to the global cancer statistics in 2020, the estimated annual cases for OSCC were 377,713 and the estimated deaths were 177,757 (Sung et al. 2021). Pathogenic factors of OSCC oftentimes involve abuse of alcohol, tobacco consumption, or both (Johnson et al. 2020). Distant metastasis is a major characteristic of OSCC and a decisive factor affecting the prognosis of patients (Irani 2016). The 5-year survival rate of patients can reach 90% if the malignance is diagnosed at the initial stage, while it would fall to less than 50% once recurrent and metastatic diseases occur (Bloebaum et al.

2014; Panzarella et al. 2014). It remains an urgent task to identify more predictive markers for an early diagnosis and more key molecules implicated in the malignant progression of tumor cells.

Transcriptional regulators are well-recognized key mediators in cell differentiation and transition, and their regulatory networks have causative correlation with tumor progression (Marengo et al. 2016; Xiong et al. 2022). In the present work, we obtained nuclear receptor interacting protein 1 (NRIP1) as a candidate transcription regulator with an aberrant expression profile in OSCC by analyzing four Gene Expression Omnibus (GEO) datasets. NRIP1, also known as RIP140, is a transcriptional coregulator that was initially identified in breast cancer cells via its interaction with estrogen receptor (Cavailles et al. 1995). It exerts crucial physiological roles by orchestrating the activity of a variety of transcription regulators (Lapierre et al. 2015). NRIP1 has been identified to be upregulated with oncogenic

Received February 2, 2023; revised and accepted April 2, 2023; J-STAGE Advance online publication April 13, 2023

Correspondence: Guangyao Hu, Department of Stomatology, Affiliated Hospital of Beihua University, No. 3999, Binjiang East Road, Fengman District, Jilin, Jilin 132011, China.

e-mail: Hugy3261@126.com

©2023 Tohoku University Medical Press. This is an open-access article distributed under the terms of the Creative Commons Attribution-NonCommercial-NoDerivatives 4.0 International License (CC-BY-NC-ND 4.0). Anyone may download, reuse, copy, reprint, or distribute the article without modifications or adaptations for non-profit purposes if they cite the original authors and source properly.

<https://creativecommons.org/licenses/by-nc-nd/4.0/>

roles in several human malignancies, such as esophageal squamous cell carcinoma (Chen et al. 2020), breast cancer (Aziz et al. 2015), and nasopharyngeal carcinoma (Chao et al. 2019). On the other hand, studies have also demonstrated the tumor suppressive effect of NRIP1 in several cases (Zhang et al. 2015; Jacquier et al. 2022a, b), indicating that it might affect tumor progression in a cellular-dependent manner. However, its expression profile and function in OSCC remain unstudied yet.

When it comes to the downstream molecules affected by NRIP1, we obtained nuclear receptor binding SET domain protein 2 (NSD2) as a target of NRIP1 and DGCR8 microprocessor complex subunit (DGCR8) as a target of NSD2 via integrated bioinformatics predictions. The reason why we focused on NSD2 is that we previously found that it promoted the malignant progression of OSCC by activating the E2F transcription factor 1 (E2F1)/Y-box binding protein 2 (YBX2) axis (Zhang and Hu 2022). NSD2, also known as MMSET or WHSC1, is a SET domain-containing protein lysine methyltransferase principally catalyzing dimethylation of histone H3 at lysine 36 (H3K36me2) that favors transcriptional activation of certain oncogenes (Kuo et al. 2011). Moreover, we further obtained via bioinformatics tools that DGCR8 shows close correlation with NSD2. DGCR8 is an RNA-binding protein that plays key roles in the biogenesis of canonical microRNAs by coordinating with the ribonuclease III enzyme Drosha, which is also closely linked to the pathogenesis of cancers (Lu et al. 2020; Mirahmadi et al. 2021). However, the exact role of DGCR8 in OSCC remains untouched. Taken together, we hypothesized that there might be an NSD/DGCR8 interaction implicated in OSCC by which NRIP1 mediates the progression of the malignancy.

## Materials and Methods

### Bioinformatics analyses

Four OSCC-related datasets (GSE9844, GSE23558, GSE25104 and GSE74530) were downloaded from the NCBI GEO system (<https://www.ncbi.nlm.nih.gov/gds/>). GSE9844 includes 26 OSCC samples and 12 normal control samples; GSE23558 contains 27 OSCC samples and 4 independent normal control samples; GSE25104 (GPL5175 platform) contains 57 OSCC samples and 22 control samples; GSE74530 includes six pairs of OSCC samples and adjacent tissue samples.

Differentially expressed genes (DEGs) between OSCC and control samples were screened using a  $p < 0.05$  threshold, and volcano plots for DEGs in each dataset were generated using Sangerbox (<http://www.sangerbox.com/tool.html>). A Venn diagram of the intersection of DEGs in the four datasets was drawn using jvenn (<http://jvenn.toulouse.inra.fr/app/example.html>). The expression patterns of NRIP1, NSD2, and DGCR8 and genes correlated with NSD2 in HNSCC were predicted using TCGA-related datasets in UALCAN (<http://ualcan.path.uab.edu/index.html>), a comprehensive analysis tool for cancer omics databases.

The downstream targets of NRIP1 were predicted in hTFtarget (<http://bioinfo.life.hust.edu.cn/hTFtarget/#/>), a comprehensive database available for the prediction of human transcription factors and their target genes. The predicted targets were cross-screened with the four sets of DEGs to obtain candidate downstream targets of NRIP1 in OSCC. The core proteins among the downstream candidates were obtained by establishing a protein-protein interaction (PPI) network using STRING system (<https://cn.string-db.org/>).

### Cell incubation

Normal human oral keratinocytes HOK (YS1199C), and human OSCC cell lines SCC-9 (YS336C), CAL-27 (YS498C) and HSC-3 (YS1645C) were procured from Yaji Biological (Shanghai, China). All cells were authenticated by short tandem repeat analysis and incubated in Dulbecco's modified Eagle's medium (D0697, Sigma-Aldrich, Merck KGaA, Darmstadt, Germany) along with 10% fetal bovine serum (FBS) and 1% antibiotics. The culture condition was maintained at 37°C with 5% CO<sub>2</sub>.

### Lentivirus-based cell infection

Lentivirus vectors carrying overexpression plasmid of NSD2 (oe-NSD2), oe-DGCR8, short hairpin (sh) RNA of NRIP1 (sh-NRIP1), sh-NSD2, and the corresponding negative control (NC; oe-NC and sh-NC) were constructed by Sangon Biotech Co., Ltd. (Shanghai, China). Exponentially growing SCC-9 and CAL-27 cells were seeded in six-well plates and infected with the lentivirus solution when the cell confluence reached approximately 60-70%. After 48 h of incubation at 37°C with 5% CO<sub>2</sub>, stably infected cells were screened by antibiotics, and the gene expression in cells was analyzed by reverse transcription quantitative polymerase chain reaction (RT-qPCR) to evaluate the infection efficacy.

### RT-qPCR

Cellular RNA was extracted using the TRIzol RNA extraction reagent (N065, Nanjing Jiancheng Bioengineering Institute, Nanjing, China) and reverse-transcribed to cDNA using the Transcriptor High Fidelity cDNA Synthesis Kit (5081955001, Sigma-Aldrich). The cDNA was amplified for real-time qPCR analysis using the KiCqStart® SYBR® Green qPCR ReadyMix™ (KCQS03, Sigma-Aldrich). The PCR primers (Table 1) were designed and synthesized using the primer designing tool (<http://www.ncbi.nlm.nih.gov/tools/primer-blast/>). Relative gene expression was evaluated by the 2<sup>-ΔΔCt</sup> method.

### Western blot analysis

Total protein in cells or xenograft tumor tissues (see details below) was extracted using the mixture of cell lysis buffer and protease inhibitor. The protein sample was separated by SDS-PAGE and transferred onto nitrocellulose membranes. The membranes were blocked with non-fat

Table 1. Primer sequences for reverse transcription quantitative polymerase chain reaction (RT-qPCR).

Gene symbol	Forward primer (5'-3')	Reverse primer (5'-3')
<i>NRIP1</i>	TGACTGAAGGAGGACAGGGA	CAAGCTCTGAGCCTCTGCTT
<i>NSD2</i>	CGCTGCAGTGTGAGTAATGC	CTGAGTTAGCCAAGAGGCC
<i>DGCR8</i>	GACAGGCTTTCCAGATGGCT	CGGAGTGGCACCTTTCTTCT
<i><math>\beta</math>-actin</i>	ACAGAGCCTCGCCTTTGCC	TGGGGTACTTCAGGGTGAGG

NRIP1, nuclear receptor interacting protein 1; NSD2, nuclear receptor binding SET domain protein 2; DGCR8, DGCR8 microprocessor complex subunit.

milk and then probed with the primary antibodies including NRIP1 (1:500, A9955, ABclonal Technology Co., Ltd., Wuhan, China), B-cell lymphoma-2 (Bcl-2; 1:500, A0208, ABclonal), Bcl-2-associated X (Bax; 1:500, A0207, ABclonal), NSD2 (1:500, GTX106306, GeneTex Inc., San Antonio, TX, USA), DGCR8 (1:1,000, ab191875, Abcam Inc., Cambridge, MA, USA), H3K36me2 (1:2,000, ab176921, Abcam), and  $\beta$ -actin (1:500, GTX109639, GeneTex) overnight at 4°C. Thereafter, the membranes were further incubated with HRP-conjugated mouse anti-rabbit IgG (1:2,000, D110065, Sangon Biotech) at room temperature for 1 h. The blot bands were developed by enhanced chemiluminescence reagent. The gray value of the protein bands was evaluated by Image J to analyze expression of target proteins.

#### Cell counting kit-8 (CCK-8) method

Treated SCC-9 and CAL-27 cells were digested and seeded in 96-well plates. At 0 h, 6 h, 12 h, 18 h, 24 h, 36 h, and 48 h, respectively, each well was added with 10  $\mu$ L CCK-8 reagent (E606335, Sangon Biotech), followed by another 2 h of incubation at 37°C. The optical density at 450 nm was read by microplate reader.

#### Colony formation assay

Treated SCC-9 and CAL-27 cells were seeded in six-well plates at  $10^3$  cells per well and cultured for 10 d. The colonies formed by cells were fixed by 4% paraformaldehyde (E672002, Sangon Biotech) for 15 min, stained with 0.1% crystal violet (A100528, Sangon Biotech), and counted under microscopy.

#### Flow cytometry

According to the instructions of the Annexin V-fluorescein isothiocyanate (FITC)/propidium iodide (PI) apoptosis detection kit (G003-1-2, Nanjing Jiancheng), the SCC-9 and CAL-27 cells were digested and resuspended. The cell suspension ( $1 \times 10^6$  cells/mL) was added to the tubes and incubated with 5  $\mu$ L Annexin V FITC and 5  $\mu$ L PI reagent at room temperature in the dark for 10 min. The apoptosis rate of cells was then analyzed by flow cytometer.

#### Transwell migration and invasion assays

Treated SCC-9 and CAL-27 cells resuspended in serum-free medium was seeded into the Transwell apical

chambers (Matrigel pre-coating was applied for invasion test), and the basolateral chambers were added with 500  $\mu$ L fresh medium containing 10% FBS. After 24 h of incubation, the migratory or invasive cells were fixed and stained with crystal violet, and the cell number was calculated under microscopy.

#### Luciferase reporter assay

The promoter sequences of NSD2 and DGCR8 were inserted in the pGL4.10 luciferase vector (E6651, Promega Corporation, Madison, WI, USA) to construct corresponding luciferase reporter vectors. The constructed vectors were transfected into SCC-9 and CAL27 cells along with sh-NRIP1, sh-NSD2, or sh-NC. After 48 h, the luciferase activity in cells was analyzed according to the protocol of the dual luciferase reporter system (E1910, Promega).

#### Chromatin-immunoprecipitation (ChIP)-qPCR

According to the instruction manual of the ChIP kit (Cat. No. 492024, Thermo Fisher Scientific, Rockford, IL, USA), the SCC-9 or CAL27 cells were cross-linked in 1% formaldehyde and ultrasonicated to truncate DNA to 200-500 bp fragments. Thereafter, the lysates were reacted with the antibodies of NRIP1 (customized by Sangon Biotech), NSD2 (1:50, ab75359, Abcam), and H3K36me2 (1:50, ab176921, Abcam) overnight for immunoprecipitation, with normal rabbit IgG (A7016, Beyotime Biotechnology Co., Ltd., Shanghai, China) or normal mouse IgG (A7028, Beyotime) used as the NC antibodies. The DNA in the immunoprecipitated complexes was eluted and purified for qPCR analysis.

#### Xenograft tumor models

Sixty male BALB/c mice (6 weeks old) were procured from Cavens Laboratory Animal Co., Ltd. (Jiangsu, China) and used in protocols approved by the Animal Ethics Committee of Affiliated Hospital of Beihua University. The animal experiment procedures also adhered to the Guide for the Care and Use of Laboratory Animals (NIH, Bethesda, MD, USA). Thirty mice were used to construct subcutaneous xenograft tumor models, and the rest 30 mice were used to analyze tumor metastasis *in vivo*.

For xenograft tumor induction, the 30 mice were allocated into sh-NC, sh-NRIP1, sh-NRIP1 + oe-NC, sh-NRIP1 + oe-NSD2, and sh-NRIP1 + oe-DGCR8 groups, n = 6 in

each. In short, 100  $\mu$ L cell suspension (containing  $1 \times 10^6$  lentivirus-infected SCC-9 cells) was injected subcutaneously at the right abdomen. The length (L) and width (W) of the tumors were examined using the caliper once a week, and the tumor volume (V) was calculated as follows:  $V = L \times W^2/2$ . After four weeks, the mice were euthanized by excessive anesthesia, and the xenograft tumor tissues were collected.

As for tumor metastasis model, the mice were also divided into the above five groups,  $n = 6$  in each. The same volume of SCC-9 cell suspension was injected into mice via tail vein. After four weeks, the mice were euthanized, and the lung tissues were collected for hematoxylin and eosin (HE) staining.

#### *Immunohistochemistry (IHC)*

Tumor tissue sections (4  $\mu$ m) were deparaffined, rehydrated, and blocked with 3%  $H_2O_2$  in methanol for 30 min. After that, the sections were incubated with anti-Ki67 (1:100, SAB5700770, Sigma-Aldrich) at 4°C overnight and then with HRP-conjugated mouse anti-rabbit IgG (1:2,000, D110065, Sangon Biotech) for 1 h. After color development by DAB kit (GTX73338, GeneTex) and counter-staining by hematoxylin, followed by microscopy observation.

#### *HE staining*

The mouse lung tissue sections (5  $\mu$ m) were deparaffined, rehydrated, and then stained with 10% hematoxylin reagent and with 0.2% glacial acetic acid containing 1% eosin. After that, the tissue sections were rehydrated again, cleared, and then sealed by neutral resin for microscopy observation.

#### *Statistical analysis*

Experimental data analysis and the histogram plotting were performed by GraphPad Prism 8 (GraphPad, La Jolla, CA, USA). All data were expressed as the mean  $\pm$  standard deviation (SD). Differences were compared by the unpaired *t* test, or by the one- or two-way analysis of variance (ANOVA) plus Tukey's post-hoc test. A *p*-value less than 0.05 was statistically significant.

## **Results**

### *NRIP1 shows a high-expression profile in OSCC*

Differentially expressed genes (DEGs) ( $p < 0.05$ ) between OSCC and control samples were identified by analyzing four OSCC-related GEO datasets (GSE9844, GSE23558, GSE25104 and GSE74530) (Fig. 1A). The DEGs screened from the four datasets were cross-analyzed via the jvenn system, with 397 common outcomes obtained (Fig. 1B). We further queried these candidate genes in the hTFtarget system and identified 17 transcription factors, amongst which NRIP1 attracted our interests as its oncogenic role has been demonstrated in several cancer types, but not in OSCC. According to data in the UALCAN system, NRIP1 is highly expression in HNSC (Fig. 1C).

Indeed, we confirmed that the mRNA and protein levels of NRIP1 were conspicuously elevated in OSCC cell lines compared to the normal HOK cells (Fig. 1D, E). The SCC-9 and CAL-27 cell lines with the highest levels of NRIP1 were selected for subsequent use.

### *Knockdown of NRIP1 suppresses the malignant phenotype of OSCC cells*

Three shRNAs of NRIP1 (sh-NRIP1 1#, 2#, and 3#) were introduced in SCC-9 and CAL-27 cells for gene knockdown, and the sh-NRIP1 1# with the best suppressive effect (Fig. 2A) was used in the subsequent assays. Under NRIP1 knockdown, both SCC-9 and CAL-27 cell lines showed significantly reduced viability and colony formation ability (Fig. 2B, C). Transwell assays also showed that the number of migratory or invasive cells was decreased (Fig. 2D, E). Moreover, flow cytometry showed that the apoptosis of the SCC-9 and CAL-27 cells was promoted by the NRIP1 knockdown (Fig. 2F), which could also be shown by the western blot assays that a decline in Bcl-2 protein and an increase in Bax protein were detected (Fig. 2G).

### *NRIP1 silencing suppresses NSD2 transcription*

We next predicted the downstream targets of NRIP1 in the hTFtarget system and had the candidate targets compared with the four sets of DEGs above, with 72 genes found intersected (Fig. 3A). A PPI network based on the 72 factors was established using the STRING system (the interaction-free factors were concealed), and the transcriptional regulation of NRIP1 on NSD2 was confirmed in the hTFtarget system (Fig. 3B). We noticed NSD2 (WHSC1) as we previously found that it played an oncogenic role in OSCC by activating the E2F1/YBX 2 axis (Zhang and Hu 2022). Similarly, NSD2 presents a high-expression profile in the UALCAN system (Fig. 3C). We validated increased NSD2 expression in the OSCC cell lines (Fig. 3D). Interestingly, in SCC-9 and CAL-27 cells induced with sh-NRIP1, reduced NSD2 mRNA was detected (Fig. 3E). The subsequent ChIP-qPCR assay revealed that the NRIP1 downregulation in cells reduced the binding of NSD2 promoter fragments with NRIP1 (Fig. 3F). Alike, the NRIP1 downregulation reduced the luciferase activity of the NSD2 promoter reporter vector in the SCC-9 and CAL-27 cells (Fig. 3G).

### *NSD2 upregulates DGCR8 through histone methylation*

To examine more molecules implicated in NSD2-mediated oncogenic events, we queried genes showing positive correlation with NSD2 in HNSC in the UALCAN system. Meanwhile, the enrichments of NSD2 and H3K36me2 in the promoters of genes of interests were queried via the Cistrome database (<http://cistrome.org/db/#/>) (Fig. 4A). DGCR8, with the closest correlation with NSD2 and with the enrichments of NSD2 and H3K36me2 in its promoter, was selected for subsequent research. DGCR8 also presents a high-expression profile in HNSC in the UALCAN

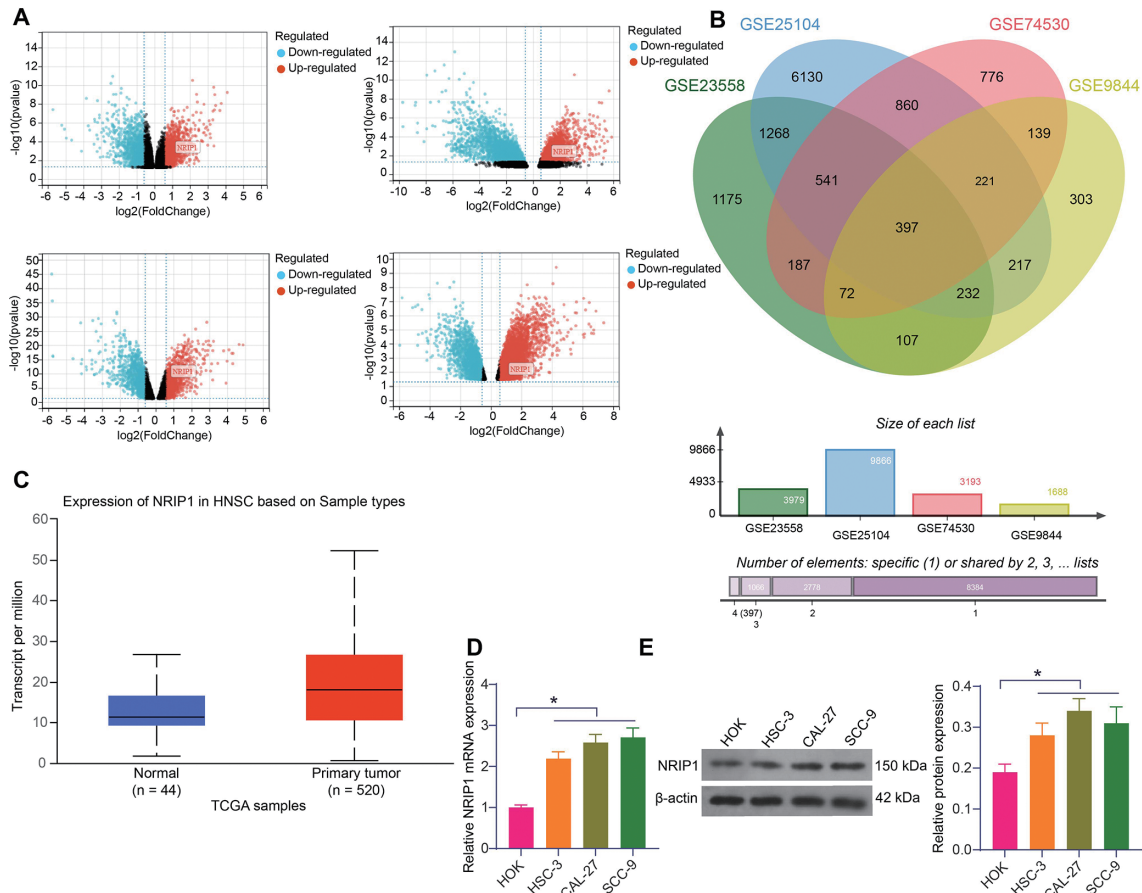


Fig. 1. NRIP1 shows a high-expression profile in oral squamous cell carcinoma (OSCC).

(A) Differentially expressed genes (DEGs) between OSCC and control samples screened from four Gene Expression Omnibus (GEO) datasets (GSE9844, GSE23558, GSE25104 and GSE74530). (B) Intersecting genes among the four sets of DEGs. (C) Transcription level of NRIP1 in head and neck squamous cell carcinoma (HNSC) ( $n = 520$ ) and normal tissues ( $n = 44$ ) in the UALCAN system (Transcripts per million). (D) mRNA and (E) protein levels of NRIP1 in OSCC cell lines and in normal HOK cells determined by RT-qPCR and western blot assays ( $n = 3$ ). Data are expressed as the mean  $\pm$  SD. Differences were compared by the  $t$  test (C) or the one-way ANOVA (D-E). \* $p < 0.05$ .

system (Fig. 4B). Indeed, elevated DGCR8 mRNA was detected in OSCC cell lines as well (Fig. 4C). We conjectured that NSD2 near the DGCR8 promoter might modulate the DGCR8 expression through histone methylation. Importantly, we introduced sh-NSD2 in the SCC-9 and CAL-27 cells, which not only suppressed the protein level of NSD2, but also led to a decline in the protein level of H3K36me2 (Fig. 4D). The RT-qPCR results also showed that the sh-NSD2 in cells resulted in decreased mRNA expression of DGCR8 (Fig. 4E). The ChIP-qPCR assay showed that the abundant DGCR8 promoter fragments bound by NSD2 or H3K36me2 were significantly reduced by NSD2 knockdown (Fig. 4F). The luciferase assay also revealed that sh-NSD2 reduced the transcriptional activity of DGCR8 (Fig. 4G). These results indicate that NSD2 can modulate H3K36me2 modification near the DGCR8 promoter to activate the DGCR8 transcription.

#### Upregulation of NSD2 or DGCR8 rescues the malignant properties of OSCC cells

In SCC-9 and CAL-27 cells, silencing of NRIP1 led to

reduced levels of NSD2 and DGCR8. Further administration of oe-NSD2 restored the NSD2 and DGCR8 levels in cells, and oe-DGCR8 rescued the DGCR8 level as well, though it did not affect the expression of NSD2 (Fig. 5A). Of note, either oe-NSD2 or oe-DGCR8 restored the viability and colony formation ability of the SCC-9 and CAL-27 cells (Fig. 5B, C) and increased cell migration and invasion (Fig. 5D, E). Flow cytometry showed that the cell apoptosis induced by NRIP1 silencing was largely blocked upon NSD2 or DGCR8 overexpression (Fig. 5F). In line, the western blot assay showed that NSD2 or DGCR8 upregulation also restored the protein level of Bcl-2 and reduced the protein level of Bax in cells (Fig. 5G). These results indicate that NRIP1 possibly mediates the NSD2/DGCR8 axis to induce OSCC progression.

#### The NRIP1/NSD2/DGCR8 axis regulates tumor growth and metastasis in vivo

The SCC-9 cells infected with sh-NRIP1 alone or with the additional oe-NSD2 or oe-DGCR8 were injected into mice to induce subcutaneous tumors. It was observed that

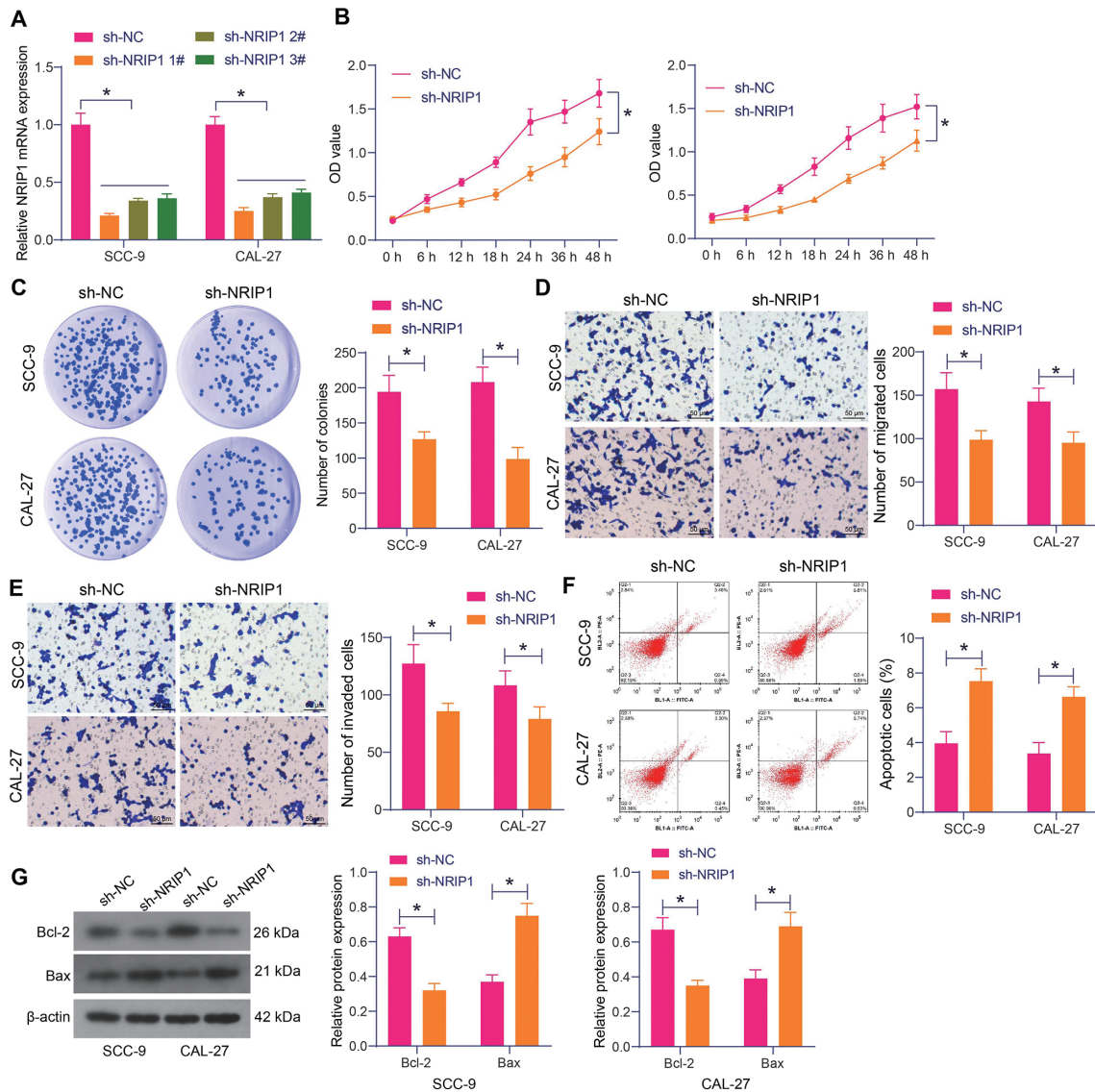


Fig. 2. Knockdown of NRIP1 suppresses the malignant phenotype of oral squamous cell carcinoma (OSCC) cells. (A) NRIP1 mRNA level in SCC-9 and CAL-27 cells after shRNA administration determined by RT-qPCR (n = 3). (B) Viability of SCC-9 and CAL-27 cells analyzed by CCK-8 assay (n = 3). (C) Colony formation ability of SCC-9 and CAL-27 cells (n = 3). (D) Migration and (E) invasion of SCC-9 and CAL-27 cells analyzed by Transwell assays (n = 3). (F) Apoptosis of SCC-9 and CAL-27 cells analyzed by flow cytometry (n = 3). (G) Protein levels of Bcl-2 and Bax in SCC-9 and CAL-27 cells determined by western blot analysis (n = 3). Differences were compared by two-way ANOVA (A-G). \* $p < 0.05$ .

the growth rate of tumors was slowed down by NRIP1 silencing but enhanced by NSD2 or DGCR8 overexpression (Fig. 6A). Moreover, the NRIP1 silencing led to reduced immunohistochemical staining of Ki67, decreased Bcl-2 but increased Bax in the xenograft tumors, but further overexpression of NSD2 or DGCR8 led to inverse trends (Fig. 6B, C). In the tail vein injection model, the HE staining showed that NRIP1 silencing decreased the number of metastatic nodules in mouse lung tissues, and the tumor metastasis was promoted by NSD2 or DGCR8 overexpression again (Fig. 6D).

## Discussion

The incidence of OSCC is particularly high in Asia-Pacific countries including China due to the betel nut chewing (Ma et al. 2022). Despite advances in the historical approaches such as surgery and chemoradiotherapy, the patient's prognosis remains unsatisfactory, especially for those with locally advanced, therapy-resistant, recurrent, and metastatic diseases (Liu et al. 2021; Wu et al. 2021). This necessitates the identification of more biomolecular mechanisms underpinning the disease progression. In the present work, the authors report a novel pathogenic network comprising the transcription regulator NRIP1, the lysine



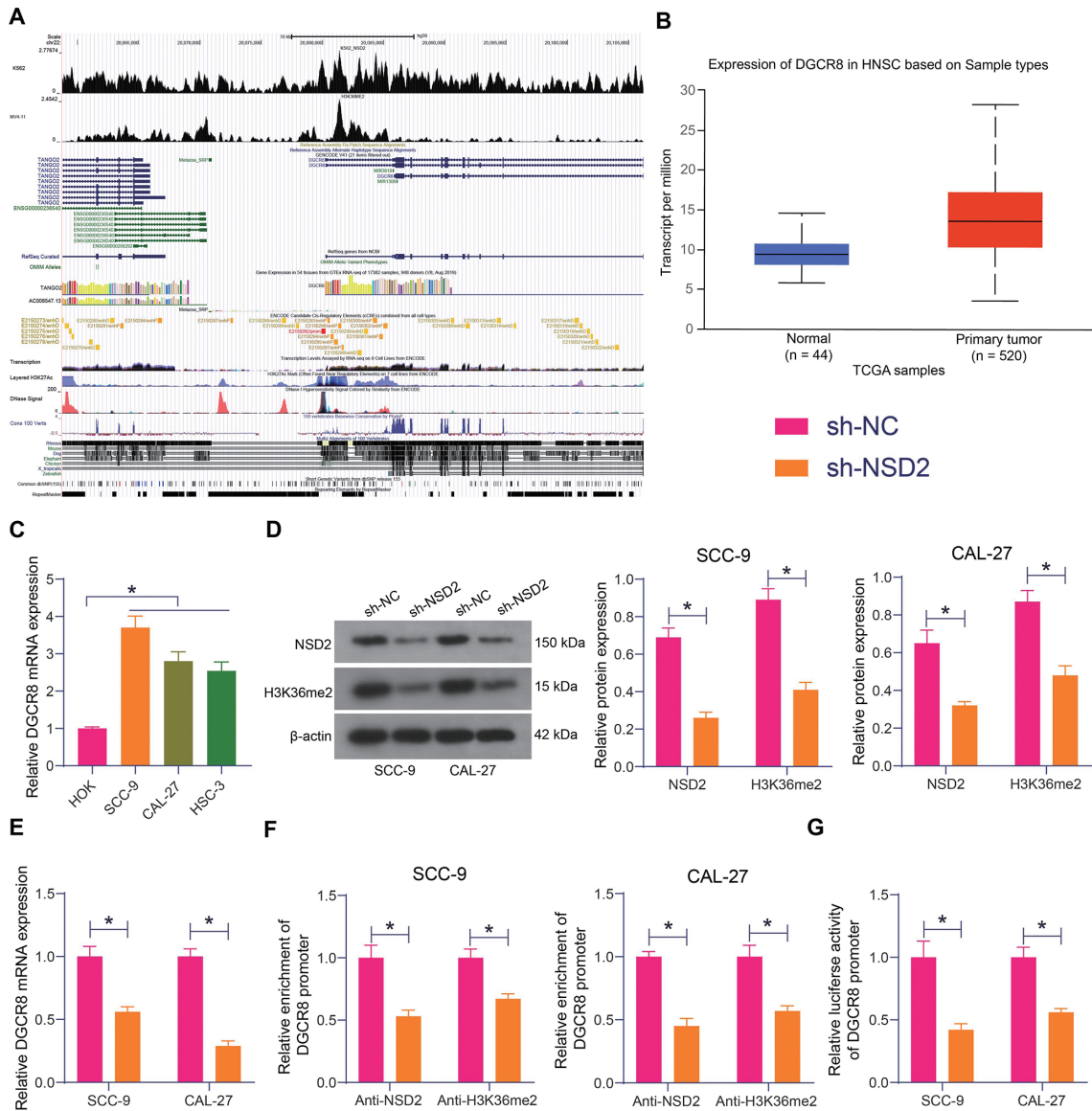


Fig. 4. NSD2 upregulates DGCR8 through histone methylation.

(A) Enrichments of NSD2 and H3K36me2 in the promoter of DGCR8. (B) Transcription level of DGCR8 in head and neck squamous cell carcinoma (HNSC) (n = 520) and normal samples (n = 44) in the UALCAN system (Transcripts per million). (C) Expression of DGCR8 in OSCC cell lines and in normal HOK cells determined by RT-qPCR (n = 3). (D) Protein levels of NSD2 and H3K36me2 in SCC-9 and CAL-27 cells administrated with sh-NSD2 determined by western blot analysis (n = 3). (E) DGCR8 mRNA expression in SCC-9 and CAL-27 cells administrated with sh-NSD2 determined by RT-qPCR (n = 3). (F) Abundance of DGCR8 promoter fragments bound with NSD2 or H3K36me2 examined by ChIP-qPCR (n = 3). (G) Binding between NSD2 and DGCR8 promoter examined by luciferase reporter gene assay (n = 3). Data are expressed as the mean  $\pm$  SD. Differences were compared by the *t* test (B), or by the one-way (C) or two-way ANOVA (D-G). \**p* < 0.05.

eral cases such as breast cancer (Jacquier et al. 2022a, b) and hepatocellular carcinoma (Zhang et al. 2015). Overall, the expression profile and function of NRIP1 in OSCC were less investigated. Here, we validated increased NRIP1 expression in OSCC cell lines and then confirmed that the artificial downregulation of NRIP1 significantly suppressed proliferation, migration and invasion, resistance to apoptosis, tumorigenicity, and *in vivo* metastatic potential of the OSCC cells. The evidence suggests that NRIP1 plays a significant oncogenic role in OSCC.

We thereafter predicted the downstream targets of NRIP1 and established a PPI network, with NSD2 identified as one of the core factors. We validated downregulated NSD2 in the OSCC cell lines and confirmed that the NSD2 upregulation rescued the malignant properties of the cells. These trends were in concert with our previous findings that NSD2 silencing blocked proliferation, invasion, and tumorigenicity of OSCC cells (Zhang and Hu 2022). By catalyzing H3K36me2, NSD2 could lead to transcriptional activation of many oncogenes and augment progression of several

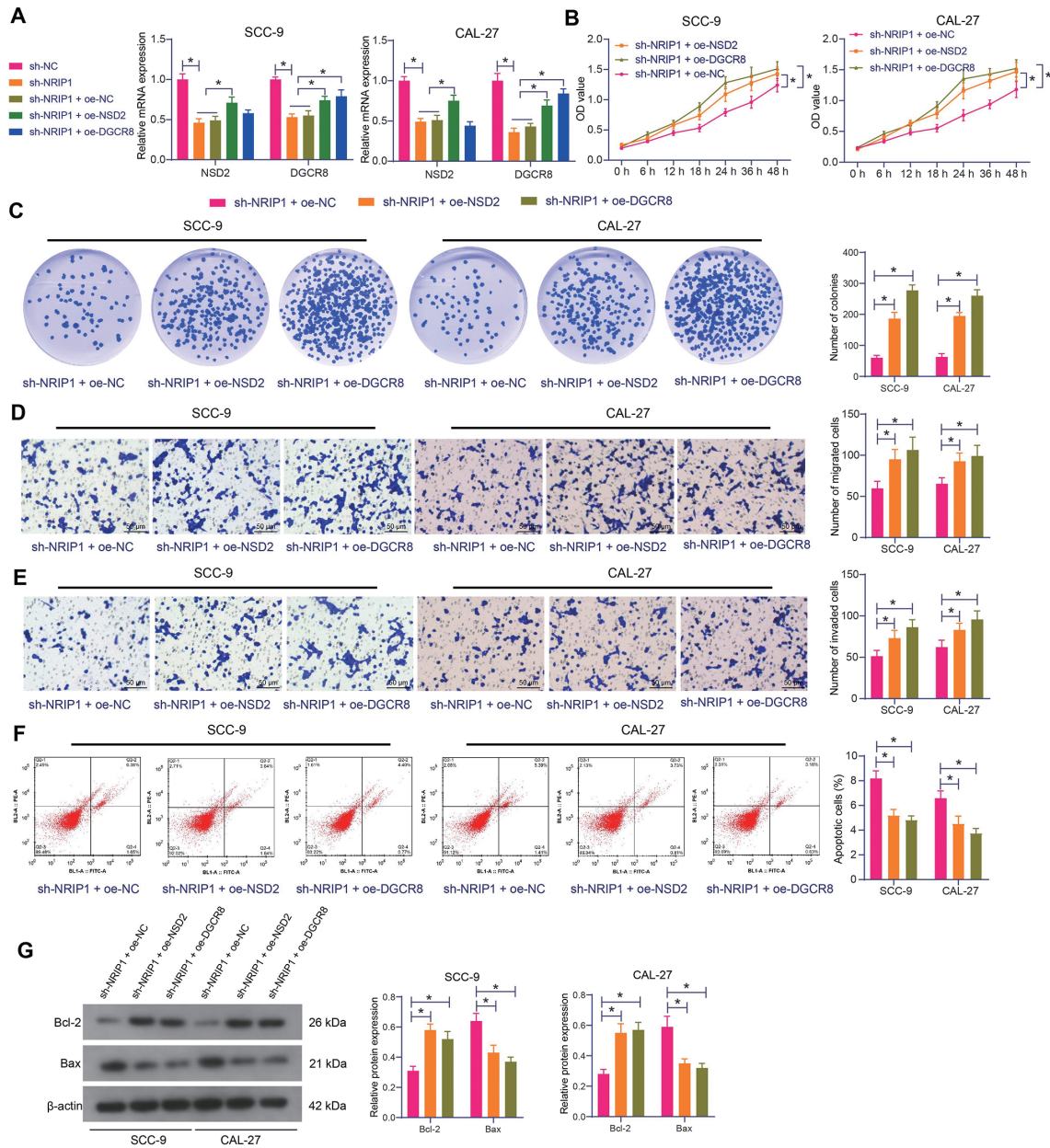


Fig. 5. Upregulation of NSD2 or DGCR8 rescues the malignant properties of oral squamous cell carcinoma (OSCC) cells. (A) NSD2 and DGCR8 expression in SCC-9 and CAL-27 cells after sh-NRIP1, oe-NSD2 or oe-DGCR8 administration determined by RT-qPCR ( $n = 3$ ). (B) Viability of SCC-9 and CAL-27 cells analyzed by CCK-8 assay ( $n = 3$ ). (C) Colony formation ability of SCC-9 and CAL-27 cells ( $n = 3$ ). (D) Migration and (E) invasion of SCC-9 and CAL-27 cells analyzed by Transwell assays ( $n = 3$ ). (F) Apoptosis of SCC-9 and CAL-27 cells analyzed by flow cytometry ( $n = 3$ ). (G) Protein levels of Bcl-2 and Bax in SCC-9 and CAL-27 cells determined by western blot analysis ( $n = 3$ ). Data are expressed as the mean  $\pm$  SD. Differences were compared by two-way ANOVA (A-G).  $*p < 0.05$ .

human malignancies (Song et al. 2021), such as colorectal cancer (Zhao et al. 2021), renal cancer (Han et al. 2020), and lung adenocarcinoma (Sengupta et al. 2021). We previously identified that the oncogenic role of NSD2 in OSCC is attributive to the activation of the E2F1/YBX2 axis (Zhang and Hu 2022). In the present work, we obtained from the UALCAN system that DGCR8 showed a strong positive correlation with NSD2. Intriguingly, high DGCR8 expression has reportedly been associated with radiosensitivity of HNSCC by upregulating microRNA-106 (Zhang et

al. 2020). However, by inducing maturation of several pri-microRNAs, the microprocessor protein has been found to enhance proliferation of tumor cells (Belair et al. 2015; Zhang et al. 2019). However, the exact function of DGCR8 in the malignant phenotype of OSCC cells remains unknown. Here, we confirmed that the NRIP1 downregulation led to a decline in DGCR8 in OSCC cells as well, and the overexpression of DGCR8 similarly restored proliferation, migration and invasion, resistance to apoptosis, tumorigenicity, and *in vivo* metastatic potential of OSCC cells as

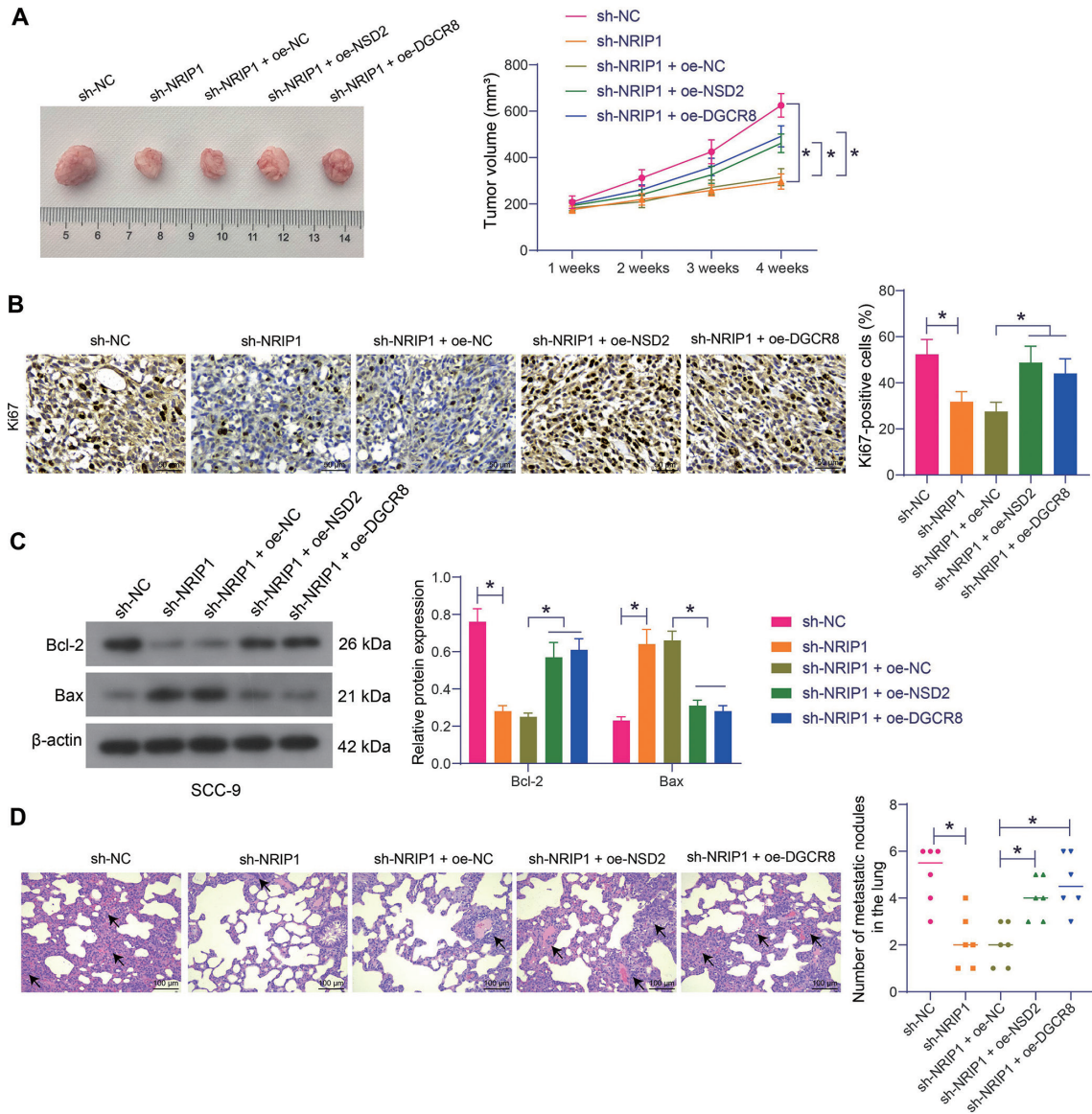


Fig. 6. The NRIP1/NSD2/DGCR8 axis regulates tumor growth and metastasis *in vivo*.

(A) Representative images of the xenograft tumors and the tumor growth rate ( $n = 6$ ). (B) Expression of Ki67 in mouse xenograft tumors examined by immunohistochemistry ( $n = 6$ ). (C) Protein levels of Bcl-2 and Bax in mouse xenograft tumors determined by western blot analysis ( $n = 6$ ). (D) Metastatic nodules in mouse lung tissues after tail vein injection of SCC-9 cells ( $n = 6$ ). Data are expressed as the mean  $\pm$  SD. Differences were compared by one-way (B, D) or two-way (A-C) ANOVA.  $*p < 0.05$ .

NSD2 did. The ample evidence demonstrates that the NSD2/DGCR8 axis is implicated in the OSCC progression mediated by NRIP1.

By the way, we previously found that the NSD2 could activate E2F1 to promote OSCC progression (Zhang and Hu 2022). Intriguingly, NRIP1 has also been reported to have close crosstalk between the E2F family members including E2F1 (Lapierre et al. 2015). Docquier et al. (2010) found that NRIP1 could suppress E2F1 transactivation on the promoters of several E2F target and inhibit the expression levels of the E2F1 targets. They further reported that the E2F1 could induce the transcription and expression of the NRIP1 gene (Docquier et al. 2012). Tsai et al. (2022)

found a similar result that the E2F1 activation increased intracellular NRIP1 levels in glioma cell lines. Therefore, it would be interesting to investigate the potential interactions between NRIP1, NSD2, and E2F1 in OSCC and perhaps in other malignancies. We would like to focus on this issue in our later research.

In summary, the present work demonstrates that NRIP1 augments malignant properties of OSCC cells by activating NSD2-mediated histone methylation of DGCR8. The findings may shed new light in the management of OSCC that suppressing any member of the NRIP1/NSD2/DGCR8 may suppress the aggressiveness of OSCC cell lines. However, there remains a major limitation of the

present work. The downstream molecules, most likely microRNAs or any signaling pathways that regulated by DGCR8, remain undefined. We would like to study on this issue in our future investigations.

### Acknowledgments

This work was supported by Science and Technology Research Project of Jilin Provincial Department of Education (JJKH20200073KJ) and 2023 Jilin Provincial Department of Education Scientific Research Project (JJKH20230084KJ).

### Conflict of Interest

The authors declare no conflict of interest.

### References

- Augereau, P., Badia, E., Balaguer, P., Carascossa, S., Castet, A., Jalaguier, S. & Cavailles, V. (2006) Negative regulation of hormone signaling by RIP140. *J. Steroid Biochem. Mol. Biol.*, **102**, 51-59.
- Aziz, M.H., Chen, X., Zhang, Q., DeFrain, C., Osland, J., Luo, Y., Shi, X. & Yuan, R. (2015) Suppressing NRIP1 inhibits growth of breast cancer cells in vitro and in vivo. *Oncotarget*, **6**, 39714-39724.
- Belair, C.D., Paikari, A., Moltzahn, F., Shenoy, A., Yau, C., Dall'Era, M., Simko, J., Benz, C. & Billelloch, R. (2015) DGCR8 is essential for tumor progression following PTEN loss in the prostate. *EMBO Rep.*, **16**, 1219-1232.
- Binato, R., Correa, S., Panis, C., Ferreira, G., Petrone, L., da Costa, I.R. & Abdelhay, E. (2021) NRIP1 is activated by C-JUN/C-FOS and activates the expression of PGR, ESRI and CCND1 in luminal A breast cancer. *Sci. Rep.*, **11**, 21159.
- Blöbaum, M., Poort, L., Bockmann, R. & Kessler, P. (2014) Survival after curative surgical treatment for primary oral squamous cell carcinoma. *J. Craniomaxillofac. Surg.*, **42**, 1572-1576.
- Castet, A., Herledan, A., Bonnet, S., Jalaguier, S., Vanacker, J.M. & Cavailles, V. (2006) Receptor-interacting protein 140 differentially regulates estrogen receptor-related receptor transactivation depending on target genes. *Mol. Endocrinol.*, **20**, 1035-1047.
- Cavaillès, V., Dauvois, S., L'Horset, F., Lopez, G., Hoare, S., Kushner, P.J. & Parker, M.G. (1995) Nuclear factor RIP140 modulates transcriptional activation by the estrogen receptor. *EMBO J.*, **14**, 3741-3751.
- Chao, C., You, J., Li, H., Xue, H. & Tan, X. (2019) Elevated SUV39H2 attributes to the progression of nasopharyngeal carcinoma via regulation of NRIP1. *Biochem. Biophys. Res. Commun.*, **510**, 290-295.
- Chen, X., Jiang, J., Zhao, Y., Wang, X., Zhang, C., Zhuan, L., Zhang, D. & Zheng, Y. (2020) Circular RNA circNTRK2 facilitates the progression of esophageal squamous cell carcinoma through up-regulating NRIP1 expression via miR-140-3p. *J. Exp. Clin. Cancer Res.*, **39**, 133.
- Docquier, A., Augereau, P., Lapierre, M., Harmand, P.O., Badia, E., Annicotte, J.S., Fajas, L. & Cavailles, V. (2012) The RIP140 gene is a transcriptional target of E2F1. *PLoS One*, **7**, e35839.
- Docquier, A., Harmand, P.O., Fritsch, S., Chanrion, M., Darbon, J.M. & Cavailles, V. (2010) The transcriptional coregulator RIP140 represses E2F1 activity and discriminates breast cancer subtypes. *Clin. Cancer Res.*, **16**, 2959-2970.
- Fang, D. & Lu, G. (2020) Expression and role of nuclear receptor-interacting protein 1 (NRIP1) in stomach adenocarcinoma. *Ann. Transl. Med.*, **8**, 1293.
- Grasedieck, S., Cabantog, A., MacPhee, L., Im, J., Ruess, C., Demir, B., Sperb, N., Rucker, F.G., Dohner, K., Herold, T., Pollack, J.R., Bullinger, L., Rouhi, A. & Kuchenbauer, F. (2022) The retinoic acid receptor co-factor NRIP1 is uniquely upregulated and represents a therapeutic target in acute myeloid leukemia with chromosome 3q rearrangements. *Haematologica*, **107**, 1758-1772.
- Han, X., Piao, L., Xu, X., Luo, F., Liu, Z. & He, X. (2020) NSD2 promotes renal cancer progression through stimulating Akt/Erk signaling. *Cancer Manag. Res.*, **12**, 375-383.
- Irani, S. (2016) Distant metastasis from oral cancer: a review and molecular biologic aspects. *J. Int. Soc. Prev. Community Dent.*, **6**, 265-271.
- Jacquier, V., Gitenay, D., Cavaillès, V. & Teyssier, C. (2022a) The transcription coregulator RIP140 inhibits cancer cell proliferation by targeting the pentose phosphate pathway. *Int. J. Mol. Sci.*, **23**, 7419.
- Jacquier, V., Gitenay, D., Fritsch, S., Bonnet, S., Gyroffy, B., Jalaguier, S., Linares, L.K., Cavaillès, V. & Teyssier, C. (2022b) RIP140 inhibits glycolysis-dependent proliferation of breast cancer cells by regulating GLUT3 expression through transcriptional crosstalk between hypoxia induced factor and p53. *Cell. Mol. Life Sci.*, **79**, 270.
- Johnson, D.E., Burtneess, B., Leemans, C.R., Lui, V.W.Y., Bauman, J.E. & Grandis, J.R. (2020) Head and neck squamous cell carcinoma. *Nat. Rev. Dis. Primers*, **6**, 92.
- Kuo, A.J., Cheung, P., Chen, K., Zee, B.M., Kioi, M., Lauring, J., Xi, Y., Park, B.H., Shi, X., Garcia, B.A., Li, W. & Gozani, O. (2011) NSD2 links dimethylation of histone H3 at lysine 36 to oncogenic programming. *Mol. Cell*, **44**, 609-620.
- Lapierre, M., Docquier, A., Castet-Nicolas, A., Gitenay, D., Jalaguier, S., Teyssier, C. & Cavailles, V. (2015) The emerging role of the transcriptional coregulator RIP140 in solid tumors. *Biochim. Biophys. Acta*, **1856**, 144-150.
- Liu, S.C., Wu, Y.C., Huang, C.M., Hsieh, M.S., Huang, T.Y., Huang, C.S., Hsu, T.N., Huang, M.S., Lee, W.H., Yeh, C.T. & Lin, C.S. (2021) Inhibition of Bruton's tyrosine kinase as a therapeutic strategy for chemoresistant oral squamous cell carcinoma and potential suppression of cancer stemness. *Oncogenesis*, **10**, 20.
- Lu, C., Zhou, D., Wang, Q., Liu, W., Yu, F., Wu, F. & Chen, C. (2020) Crosstalk of microRNAs and oxidative stress in the pathogenesis of cancer. *Oxid. Med. Cell. Longev.*, **2020**, 2415324.
- Ma, L., Shen, T., Peng, H., Wu, J., Wang, W. & Gao, X. (2022) Overexpression of PTPRZ1 regulates p120/beta-catenin phosphorylation to promote carcinogenesis of oral submucous fibrosis. *J. Oncol.*, **2022**, 2352360.
- Marengo, B., Nitti, M., Furfaro, A.L., Colla, R., Ciucis, C.D., Marinari, U.M., Pronzato, M.A., Traverso, N. & Domenicotti, C. (2016) Redox homeostasis and cellular antioxidant systems: crucial players in cancer growth and therapy. *Oxid. Med. Cell. Longev.*, **2016**, 6235641.
- Mirahmadi, Y., Nabavi, R., Taheri, F., Samadian, M.M., Ghale-Noie, Z.N., Farjami, M., Samadi-Khouzani, A., Yousefi, M., Azhdari, S., Salmaninejad, A. & Sahebkar, A. (2021) MicroRNAs as biomarkers for early diagnosis, prognosis, and therapeutic targeting of ovarian cancer. *J. Oncol.*, **2021**, 3408937.
- Panzarella, V., Pizzo, G., Calvino, F., Compilato, D., Colella, G. & Campisi, G. (2014) Diagnostic delay in oral squamous cell carcinoma: the role of cognitive and psychological variables. *Int. J. Oral Sci.*, **6**, 39-45.
- Sengupta, D., Zeng, L., Li, Y., Hausmann, S., Ghosh, D., Yuan, G., Nguyen, T.N., Lyu, R., Caporicci, M., Morales Benitez, A., Coles, G.L., Kharchenko, V., Czaban, I., Azhibek, D., Fischle, W., et al. (2021) NSD2 dimethylation at H3K36 promotes lung adenocarcinoma pathogenesis. *Mol. Cell*, **81**, 4481-4492 e4489.
- Song, D., Lan, J., Chen, Y., Liu, A., Wu, Q., Zhao, C., Feng, Y.,

- Wang, J., Luo, X., Cao, Z., Cao, X., Hu, J. & Wang, G. (2021) NSD2 promotes tumor angiogenesis through methylating and activating STAT3 protein. *Oncogene*, **40**, 2952-2967.
- Sung, H., Ferlay, J., Siegel, R.L., Laversanne, M., Soerjomataram, I., Jemal, A. & Bray, F. (2021) Global Cancer Statistics 2020: GLOBOCAN estimates of incidence and mortality worldwide for 36 cancers in 185 countries. *CA Cancer J. Clin.*, **71**, 209-249.
- Tsai, H.C., Wei, K.C., Chen, P.Y., Huang, C.Y., Chen, K.T., Lin, Y.J., Cheng, H.W., Huang, C.H. & Wang, H.T. (2022) Receptor-interacting protein 140 enhanced temozolomide-induced cellular apoptosis through regulation of E2F1 in human glioma cell lines. *Neuromolecular Med.*, **24**, 113-124.
- Wu, C.N., Wu, S.C., Chen, W.C., Yang, Y.H., Chin, J.C., Chien, C.Y., Fang, F.M., Li, S.H., Luo, S.D. & Chiu, T.J. (2021) Angiotensin II receptor blockers and oral squamous cell carcinoma survival: a propensity-score-matched cohort study. *PLoS One*, **16**, e0260772.
- Xiong, A., Zhang, J., Chen, Y., Zhang, Y. & Yang, F. (2022) Integrated single-cell transcriptomic analyses reveal that GPNMB-high macrophages promote PN-MES transition and impede T cell activation in GBM. *EBioMedicine*, **83**, 104239.
- Yang, Z., Yan, G., Zheng, L., Gu, W., Liu, F., Chen, W., Cui, X., Wang, Y., Yang, Y., Chen, X., Fu, Y. & Xu, X. (2021) YKT6, as a potential predictor of prognosis and immunotherapy response for oral squamous cell carcinoma, is related to cell invasion, metastasis, and CD8+ T cell infiltration. *Oncoimmunology*, **10**, 1938890.
- Zhang, C., Chen, H., Deng, Z., Long, D., Xu, L. & Liu, Z. (2020) DGCR8/miR-106 axis enhances radiosensitivity of head and neck squamous cell carcinomas by downregulating RUNX3. *Front. Med. (Lausanne)*, **7**, 582097.
- Zhang, D., Wang, Y., Dai, Y., Wang, J., Suo, T., Pan, H., Liu, H., Shen, S. & Liu, H. (2015) Downregulation of RIP140 in hepatocellular carcinoma promoted the growth and migration of the cancer cells. *Tumour Biol.*, **36**, 2077-2085.
- Zhang, J., Bai, R., Li, M., Ye, H., Wu, C., Wang, C., Li, S., Tan, L., Mai, D., Li, G., Pan, L., Zheng, Y., Su, J., Ye, Y., Fu, Z., et al. (2019) Excessive miR-25-3p maturation via N(6)-methyladenosine stimulated by cigarette smoke promotes pancreatic cancer progression. *Nat. Commun.*, **10**, 1858.
- Zhang, L. & Hu, G. (2022) NSD2 activates the E2F transcription factor 1/Y-box binding protein 2 axis to promote the malignant development of oral squamous cell carcinoma. *Arch. Oral Biol.*, **138**, 105412.
- Zhao, L.H., Li, Q., Huang, Z.J., Sun, M.X., Lu, J.J., Zhang, X.H., Li, G. & Wu, F. (2021) Identification of histone methyltransferase NSD2 as an important oncogenic gene in colorectal cancer. *Cell Death Dis.*, **12**, 974.
- Zschiegdrich, I., Hardeland, U., Kronen-Herzig, A., Berriel Diaz, M., Vegiopoulos, A., Muggenburg, J., Sombroek, D., Hofmann, T.G., Zawatzky, R., Yu, X., Gretz, N., Christian, M., White, R., Parker, M.G. & Herzig, S. (2008) Coactivator function of RIP140 for NFkappaB/RelA-dependent cytokine gene expression. *Blood*, **112**, 264-276.
-